ROBERT HOFSTADTER

The electron-scattering method and its application to the structure of nuclei and nucleons

Nobel Lecture, December 11, 1961

I am very conscious of the high honor that has been conferred on me and I wish to thank the Swedish Academy of Sciences sincerely for this recognition. It is a privilege and a pleasure to review the work which has brought me here and which concerns a very old and interesting problem.

Over a period of time lasting at least two thousand years, Man has puzzled over and sought an understanding of the composition of matter. It is no wonder that his interest has been aroused in this deep question because all objects he experiences, including even his own body, are in a most basic sense special configurations of matter. The history of physics shows that whenever experimental techniques advance to an extent that matter, as then known, can be analyzed by reliable and proved methods into its «elemental» parts, newer and more powerful studies subsequently show that the «elementary particles» have a structure themselves. Indeed this structure may be quite complex, so that the elegant idea of elementarity must be abandoned. This observation provides the theme of our lecture.

In recent times the structure of matter has been shown to arise from various combinations of the «atoms» of the Periodic System. The picture of the now-familiar atom was first sketched by Rutherford, Bohr, Pauli, etc., and later developed in great detail by many of their colleagues. The efforts of these scientists have led to an understanding of the cloud of electrons which surrounds the dense center of the atoms, the so-called nucleus. In the nucleus practically all the mass of the atom resides in an extremely concentrated form. The nucleus itself was an invention of the aforementioned physicists and in the year 1919 the first vague ideas concerning the sizes of nuclei were worked out. By studying the deviations from Coulomb scattering of alpha particles Rutherford showed that a nuclear radius was of the order of 105 times smaller than an atomic radius. Subsequently other investigators demonstrated by means of studies of α-particle radioactivity, neutron capture cross sections, and comparisons of the energy of decay of mirror nuclei that consistent values of nuclear size parameters could be measured.

All useful methods showed that if a nucleus could be represented by a model of a uniformly charged sphere the radius *(R)* of the sphere would be given by the relation

$$10^{-13} A^{\frac{1}{3}} \text{ cm} \qquad (1)$$

where *A* is the mass number of the nucleus.

This is the point from which the present studies began. Although much of what we wish to say will concern nucleon structure (nucleon = proton or neutron) the method of investigation we have employed had its origins in the study of larger nuclei. Consequently a historical approach beginning with the larger nuclei seems not only natural but also may be didactically sound. We shall therefore review briefly the method used in studying nuclear sizes and shall at the same time give some of the results, which may not be without interest themselves.

We have used the method of high-energy electron scattering. In essence the method is similar to the Rutherford scattering technique, but in the case of electrons it is presently believed that only a «simple» and well-understood interaction - the electromagnetic or Coulomb interaction - is involved between the incident electron and the nucleus investigated. Under these conditions quantum electrodynamics and Dirac theory teach us how to calculate a differential elastic scattering cross section. It can be shown that the differential cross section corresponding to a beam of electrons scattering against a point nucleus of small charge Ze, lacking spin and magnetic moment, is calculable by the Born approximation and takes a form:

$$\left(\frac{Ze^2}{2E}\right)^2 \frac{\cos^2 \theta/2}{\sin^4 \theta/2} \frac{}{1 + \frac{2E}{M} \sin^2 \theta/2} \qquad (2)$$

in the laboratory system of coordinates. This is the «Mott» scattering cross section where E is the incident energy, θ the scattering angle and M the mass of the struck nucleus. Other symbols in Eq. 2 have their usual meanings. if a nucleus has a finite size, and is thus not merely a point, the scattering cross section is decreased below the value of the scattering from a point. The can be described in terms of a factor, represented by F, which is called «form factor» or «structure factor ». Thus, in Born approximation,

$$_{NS} F^2 (a)$$

and this is the elastic scattering cross section for a finite nucleus". Here q is the momentum-energy transfer, defined by the relation

$$q = \frac{(2E/\hbar c)\sin\theta/2}{\sqrt{1 + (2E/Mc^2)\sin^2\theta/2}} \qquad (4)$$

The parameter q is relativistically invariant and is a very important quantity in electron-scattering studies. The form factor, F, takes account of the interference between scattered wavelets arising from different parts of the same, finite, nucleus and therefore is responsible for diffraction effects observed in the angular distribution. The quantity F is actually given by

$$F = \frac{4\pi}{q}\int_0^\infty \varrho\,(r)\,(\sin\ qr)\,r\,dr \qquad (5)$$

in the event that the nucleus exhibits spherical symmetry. The quantity $\varrho\,(r)$ is the electric charge density function, in which r represents the distance from the center of the nucleus to the volume element where ϱ is measured. A mathematical inversion of Eq. 5 allows one to deduce the form of $\varrho\,(r)$ if $F\,(q)$ is known over a large range of values of q.

Of course, since we used the Born approximation and therefore specified small values of the atomic number, the above description of the basic formulae of the electron-scattering process is only an approximate one. More exact methods of finding the scattering cross section have been developed by many authors[3]. These calculations of more precise types employ the « phase-shift » methods and are applicable to heavy nuclei as well as light ones. The qualitative physical ideas involved in the determination of nuclear structure can be adequately described by the Born approximation method (Eq. 3). Nevertheless, quantitative results definitely require the more elaborate phase-shift methods and simple, and in this case, closed formulae cannot be given to describe the scattering cross section.

Early electron-scattering experiments were carried out at the University of Illinois in 1951[4] at an incident electron energy of about 15.7 MeV. Such experiments showed that nuclear radii obeyed an approximate relationship of the type given in Eq. 1. However, few details of nuclear shape or size could be discerned because the energy of the electrons was relatively low and the corresponding De Broglie wavelength of the electrons was larger than a typical size of the nucleus. In 1953 higher energy electrons became

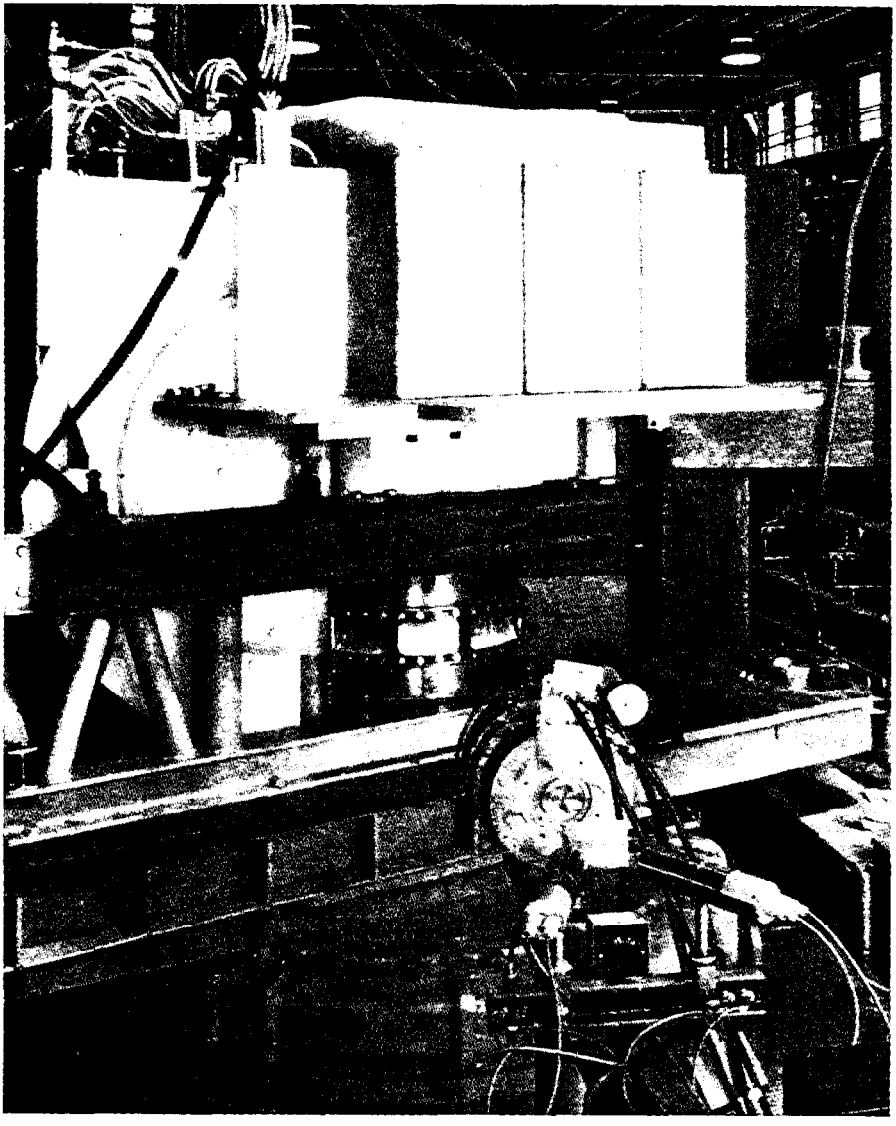

Fig. 1. The first electron-scattering apparatus built at Stanford University. The semi-circular 190-MeV spectrometer is shown at the left on its gun-mount support. The upper platform carries lead and paraffin shielding that encloses the Čerenkov counter. The brass scattering chamber is shown below with the thin window encircling it. Early forms of electron monitors appear in the foreground. The spectrometer itself is about four feet high.

available at Stanford University and at the University of Michigan and experiments on various nuclei were carried out[5]. Phase-shift interpretations of the Stanford experiments[6] showed that the rule expressed in Eq. 1 was approximately true, but that in reality the nuclear charge density distribution could not be described in terms of a single size parameter *R*. If one attempted to do so, only at the expense of an inferior fit between experiment and theory, the resulting *R* would have to be made 20% smaller than the value of the radius in Eq. 1. Mu-mesonic atom studies[7] showed, a bit earlier, that a similar conclusion was required for a one-parameter description of the size of the nucleus. Two parameters could not be determined from the mu-mesonic atom investigations.

Fig. 1 shows a photograph of the first high-energy electron-scattering equipment. This apparatus gave the above results and was employed up to an energy of about 190 MeV. An obsolete naval-gun mount was used as the rotating platform for the heavy equipment, weighing about 5 tons. The type of geometry employed in a modern electron-scattering experimental area is shown in Fig. 2. A photograph of the corresponding magnetic spectrometers and associated equipment is shown in Fig. 3. A larger form of gun mount is used again to carry the spectrometers, whose total weight is approximately

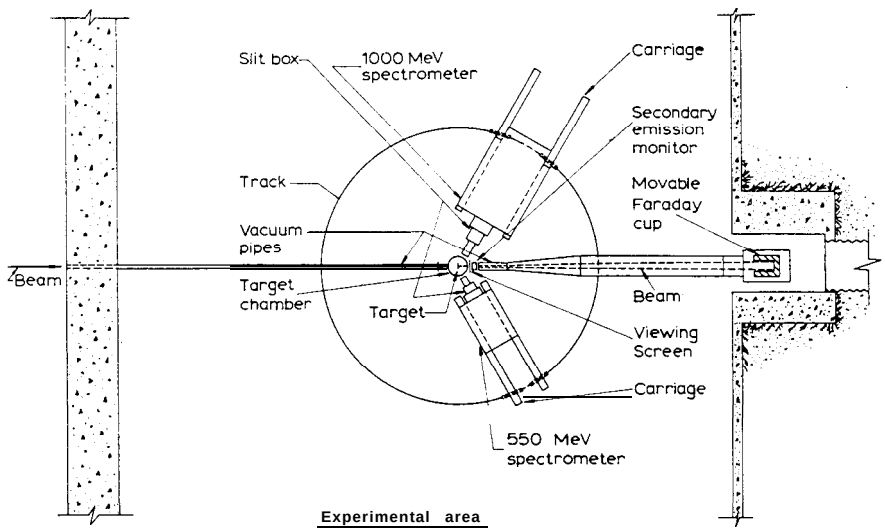

Fig. 2. This figure shows a schematic diagram of a modern electron-scattering experimental area. The track on which the spectrometers roll has an approximate radius of 13.5 feet.

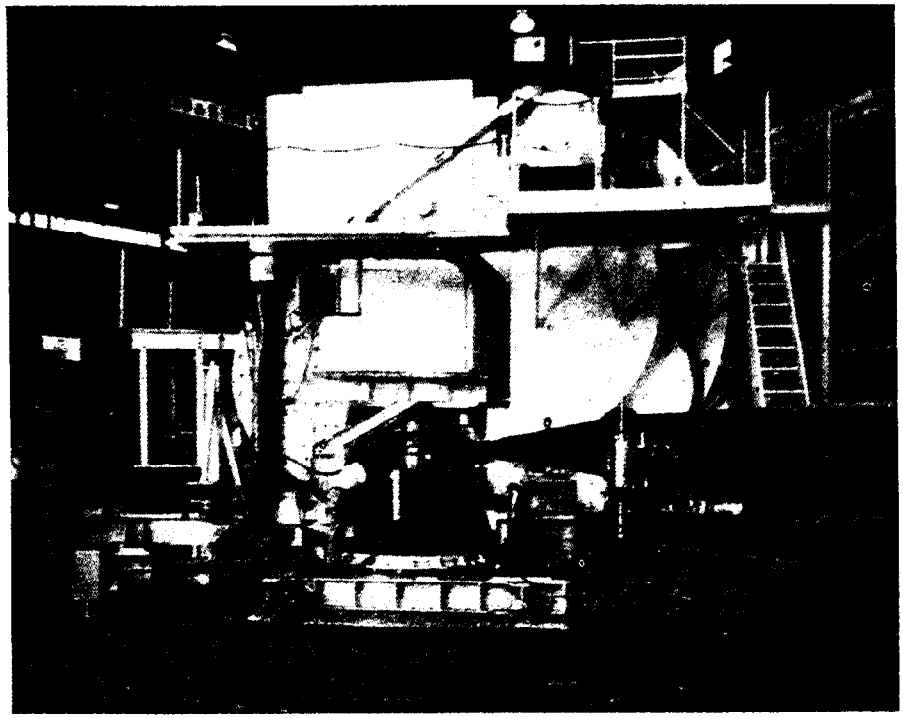

Fig. 3. A recent photograph of the double-spectrometer system is shown in this figure. The shield of the smaller spectrometer can be removed easily with the aid of an auxiliary stand, not shown in the photograph. The long tube in the foreground is the vacuum pipe leading to the Faraday cup, which is not visible in the photograph.

250 tons. Each of the two magnetic spectrometers in this apparatus is similar to the well-known Siegbahn double-focussing instrument. The two spectrometers may be used in coincidence experiments as well as « in parallel ». The massive equipment of Fig. 3 can bend and focus 1.0-BeV electrons and is required in order to resolve the elastic-scattering process from the many types of inelastic-scattering processes occurring in electron-nucleus collisions. An example of the resolution obtained in early experiments is shown in Fig. 4 in the case of a carbon target[8]. When an angular distribution in carbon is measured one may observe, e.g. in Fig. 5, the position of a diffraction minimum. The value of the angle at this minimum gives immediately an indication of the nuclear size if one employs results similar to Eqs. 2-5, when modified appropriately in terms of the phase-shift method. The solid line in the figure shows the result of a theoretical calculation of the scattering cross

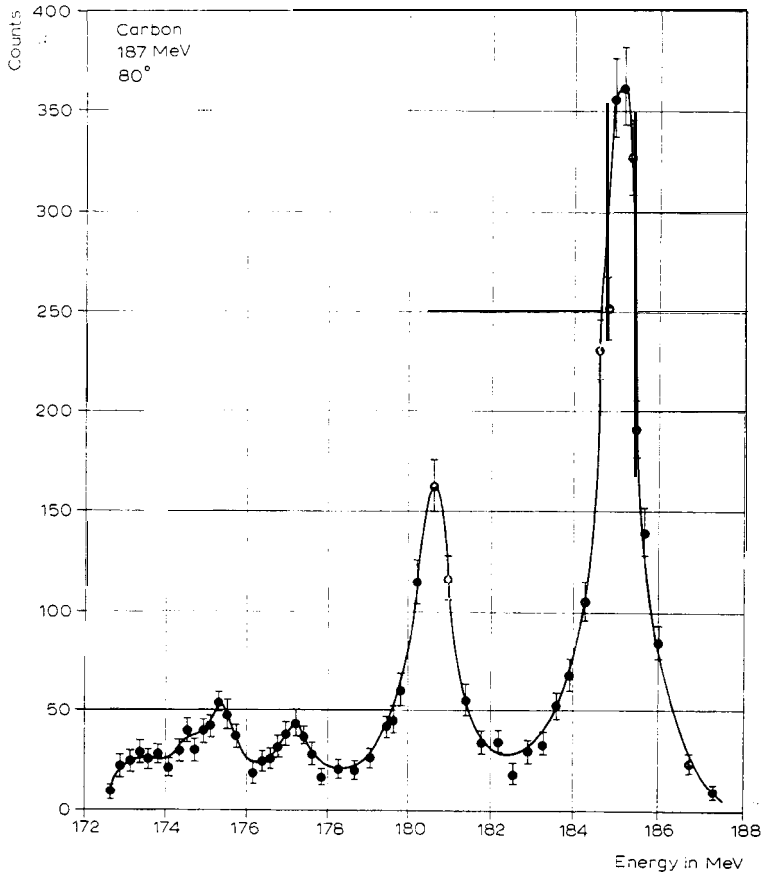

Fig. 4. This figure[8] shows the elastic-scattering peak from carbon at an abscissa near 185 MeV, and the inelastic-scattering peaks from the excited states of ^{12}C. The peak near 180.7 MeV is associated with the 4.43-MeV level.

section. From the theoretical calculation one may deduce the charge density distribution, which may be seen in Fig. 8. It is clear that a study of the inelastic-scattering peaks corresponding to the excited states of ^{12}C (or other nuclei) can be studied by the electron-scattering method. In fact, Fig. 5 shows also the angular dependence of the scattering of the 4.43-MeV level in ^{12}C. The subject of inelastic level scattering is not relevant to our present topic and we shall not pursue this matter any further in this lecture.

One last example is shown in the case of the nucleus of the gold atom. The elastic electron scattering was studied at the four different energies shown in Fig. 6. The solid lines again show the results of theoretical calculations from

which the charge density distribution, ϱ, can be obtained. This charge distribution is shown in Fig. 8.

The electron-scattering method was employed in the manner we have described and resulted in the determination of two-parameter descriptions of nuclear charge density distributions. Studies of the charge density dis-

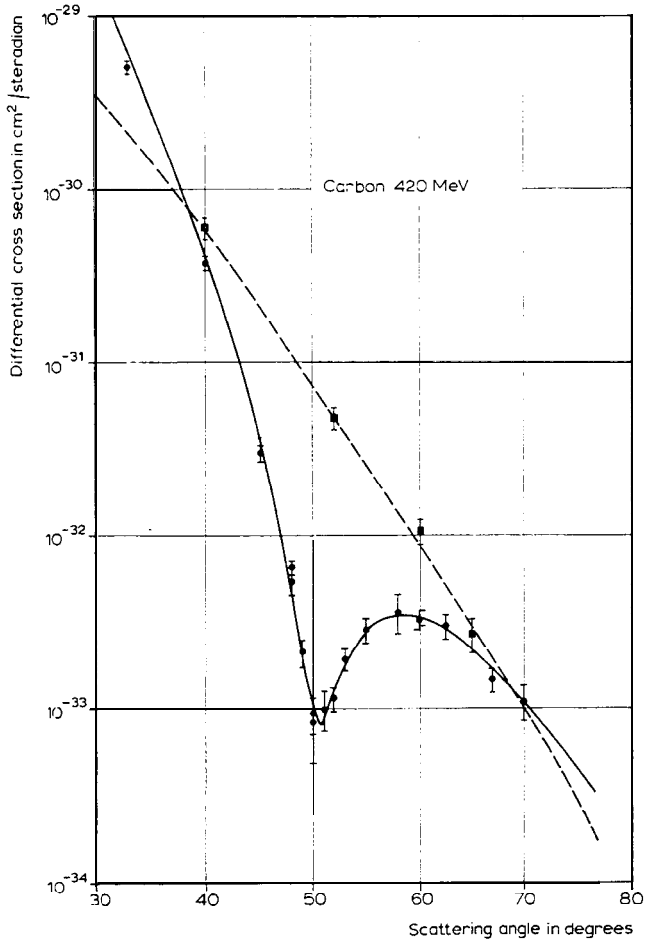

Fig. 5. This figure shows the elastic and inelastic curves corresponding to the scattering of 420-MeV electrons by ^{12}C. The *solid circles,* representing experimental points, show the elastic-scattering behavior while the *solid squares* show the inelastic-scattering curve for the 4.43-MeV level in carbon. The *solid line* through the elastic data shows the type of fit that can be calculated by phase-shift theory for the model of carbon shown in Fig. 8.

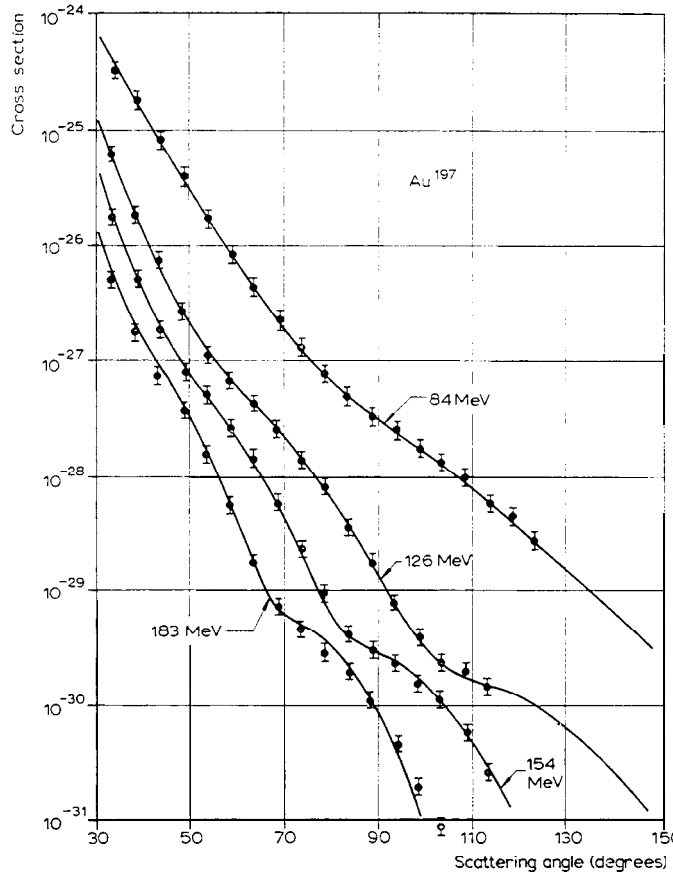

Fig. 6. The *points* represent experimental data observed by scattering electrons of the appropriate incident energies from gold nuclei[9]. The *solid lines* are calculated angular distributions for a model of the gold nucleus similar to that shown in Fig. 8.

tributions in various nuclei culminated in the evolution of a simple scheme of construction of most spherical nuclei[9]. Such nuclei could be represented by a charge density function of the type shown in Fig. 7. The exact shape of this density function is not of overriding importance; rather the distance (c) from the center of the nucleus to the 50 per cent point, and the interval (t) between the 90 per cent and 10 per cent ordinates, are the two important parameters that determine the behavior of the scattering cross sections. A trapezoidal distribution with the same values of the two parameters would also suffice to describe the experimental results in the medium and heavier nuclei when the fitting procedure is limited by the accuracy obtained in the

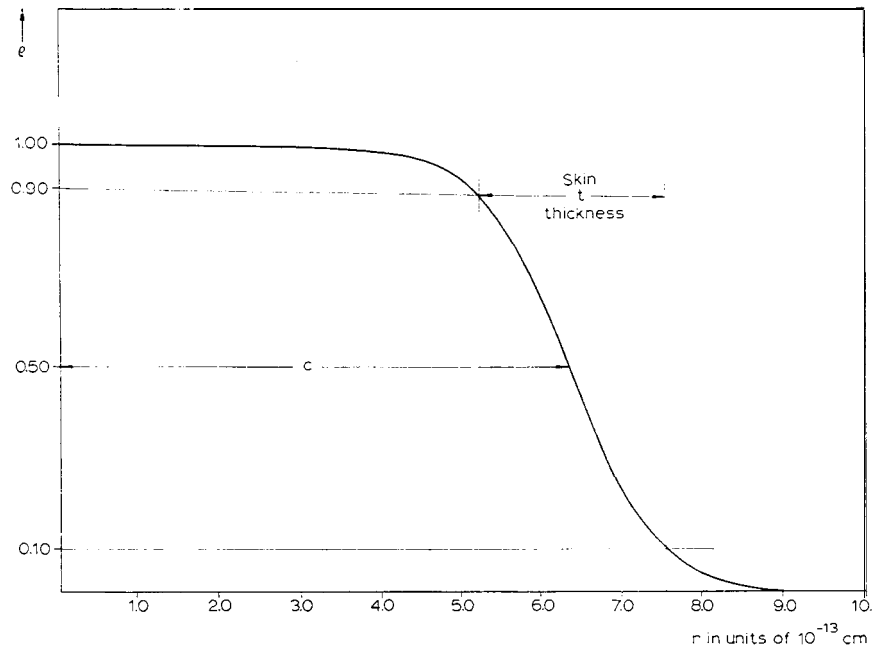

Fig. 7. The shape and parameters which describe an approximate model of the gold nucleus. This type is called the Fermi model[9].

experiments. Higher accuracy can probably distinguish between these possibilities but such studies are only beginning now.

The results of many of the above experiments covered a large range of nuclei and demonstrated[9] that two simple rules can be used to summarize the scheme of construction of spherical nuclei, viz. :

$$\begin{aligned} c &= (1.07 \pm 0.02) \cdot 10^{-13} A^{\frac{1}{3}} \text{ cm} \\ t &= (2.4 \pm 0.3) \cdot 10^{-13} \text{ cm} = \text{constant} \end{aligned} \qquad (6)$$

The first equation gives the principal parameter governing the size of a nucleus and describes the behavior with increasing A of a kind of « mean » nuclear radius. The second equation states that the nuclear skin thickness is constant. The second rule implies that there is some property of nuclear matter that causes the outer nuclear regions to develop an essentially constant surface thickness. The two rules together are responsible for the approximate constancy of the central charge density of nuclei. The latter property is il-

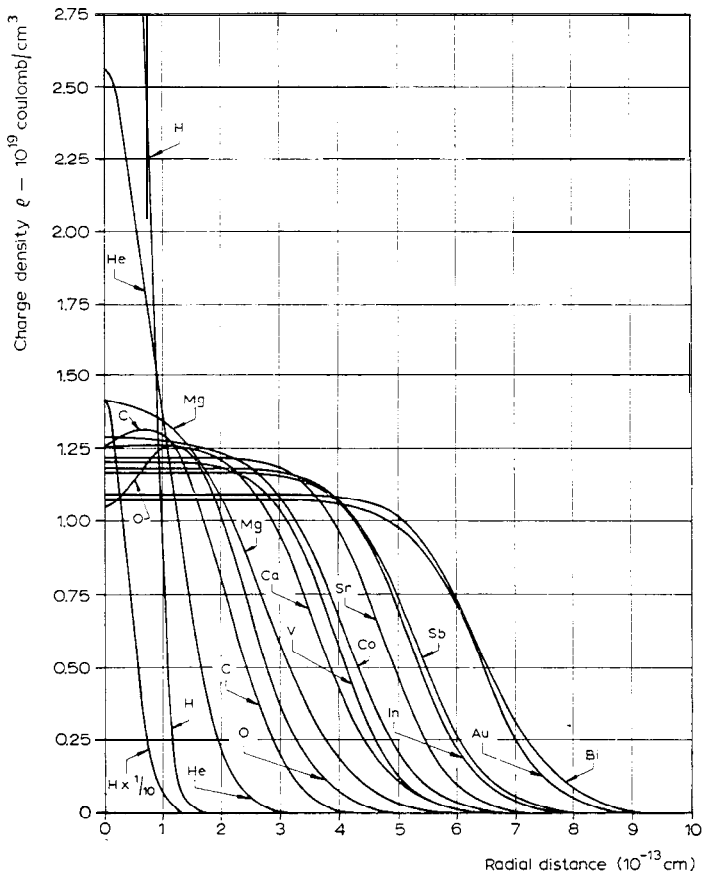

Fig. 8. This figure gives a summary of the approximate charge density distributions found for various nuclei studied by electron-scattering methods. The central densities are the least well determined positions of the curves. Note, however, the large disparity between the *average* central densities of the proton and all other nuclei. The alpha particle (^{4}He) is also a unique case and exhibits a much larger central density than all heavier nuclei.

lustrated in Fig. 8, where a summary of the charge distributions found by the electron-scattering method is presented for various nuclei. Except for the extremely light nuclei of hydrogen and helium the constancy of the central nuclear density is clearly represented in the figure.

The results obtained with heavier nuclei indicated that the electron-scattering method could also be applied to the very light nuclei and even to the proton itself. Accordingly, in early 1954 experiments were initiated on hy-

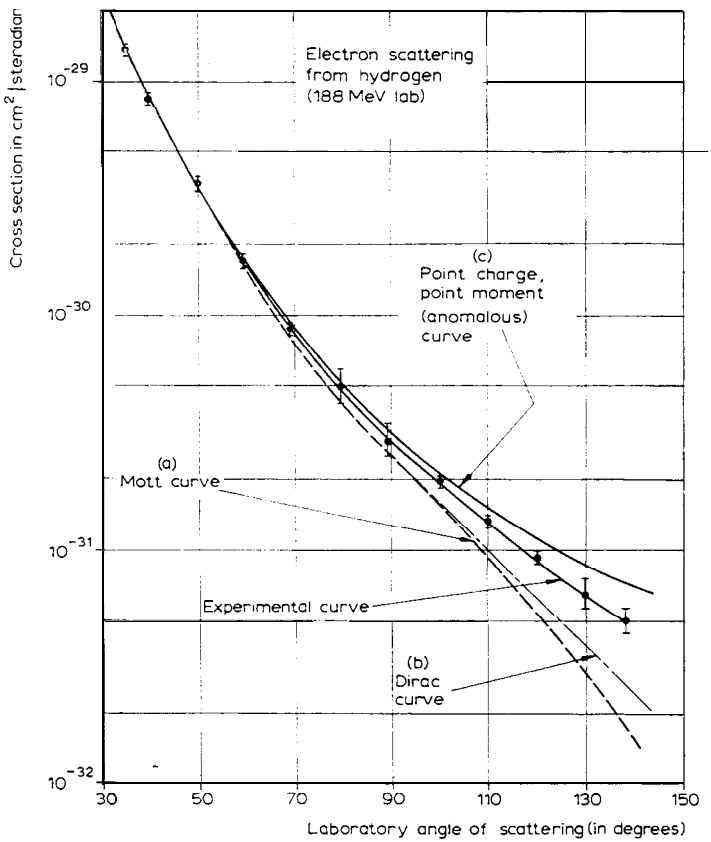

Fig. 9. Electron scattering from the proton at an incident energy of 188 MeV. *Curve (a)* shows the theoretical Mott curve for a spinless point proton. *Curve (b)* shows the theoretical curve for a point proton with a Dirac magnetic moment alone. *Curve* (*c*) shows the theoretical behavior of a point proton having the anomalous Pauli contribution in addition to the Dirac value of the magnetic moment. The deviation of the experimental curve from the Curve (*c*) represents the effect of form factors for the proton and indicates structure within the proton. The best fit in this figure indicates an rms radius close to $0.7 \cdot 10^{-13}$ cm.

drogen and helium. The first targets employed high-pressure, thin-wall, gas chambers and were designed by the late Miss Eva Wiener. In the latter part of 1954 it was first realized that the experiments on hydrogen demonstrated that the proton was an object of finite size and not merely a point object. In fact, the size was found to be surprisingly large[10] and could be described in terms of a root-mean-square radius of value $(0.74 \pm 0.24) \cdot 10^{-13}$ cm. It is an interesting fact that more recent determinations of the rms proton charge

radius appear to converge on a value of $(0.79 \pm 0.08) \cdot 10^{-13}$ cm. Fig. 9 shows the first evidence of finite size in the proton. The figure has been drawn from Ref. 10. The first experiments leading to the above conclusions were carried out at relatively low energies (~ 190 MeV).

Now the proton is known to have a spin and a magnetic moment. The magnetic moment will affect the scattering behavior appreciably at values of q (Eq. 4) in the range equal to or larger than about $0.2\ Mc$, where M is the mass of a nucleon. The magnetic type of scattering causes a leveling off in the decrease of the elastic cross section as a function of the scattering angle at high energies of the incident electrons. As we may see in Fig. 9, the experimental data fell below the expected theoretical curve for a proton possessing a point charge and a point magnetic moment. This behavior can be understood in terms of the theoretical scattering law developed by M. Rosenbluth[11] in 1950. This law described the composite effect of charge and magnetic moment scattering and is given by:

$$\frac{d\sigma}{d\Omega} = \sigma_{NS}\left\{F_1^2 + \frac{\hbar^2 q^2}{4 M^2 c^2}\left[2\,(F_1 + KF_2)^2 \tan^2 \theta/2 + K^2 F_2^2\right]\right\} \qquad (7)$$

where σ_{NS} is taken from Eq. 2 with Z = 1. In the Rosenbluth equation the quantity $F_1(q)$ is the Dirac form factor, representing the proton's charge and its associated Dirac magnetic moment. The quantity $F_2(q)$ is the Pauli form factor and represents the anomalous magnetic moment of the proton. K in the above equation indicates the static value (1.79) of the anomalous magnetic moment in nuclear magnetons.

Although one may speak qualitatively of size and shape factors of the proton in the low-energy limit it is more consistent and more desirable, from a quantitative point of view, to discuss only the two phenomenological form factors $F_1(q)$ and $F_2(q)$. Actually all the electromagnetic structure of the proton is, in principle, described by the behavior of these quantities as functions of q. Note that for the proton, $F_1(0) = F_2(0) = 1.00$. Meson theory should be able to make definite assertions about F_1 and F_2 starting from the above values. In our subsequent discussion we shall concentrate on determining the two phenomenological quantities (F_1, F_2) from the experimental data so that the form factors can be compared with theory. The experimental determinations of the form factors can be accomplished, for example, by using the method of intersecting ellipses[12] or by other equivalent methods based on the relativistic idea that each F is a function *only* of q and not of E or θ separately.

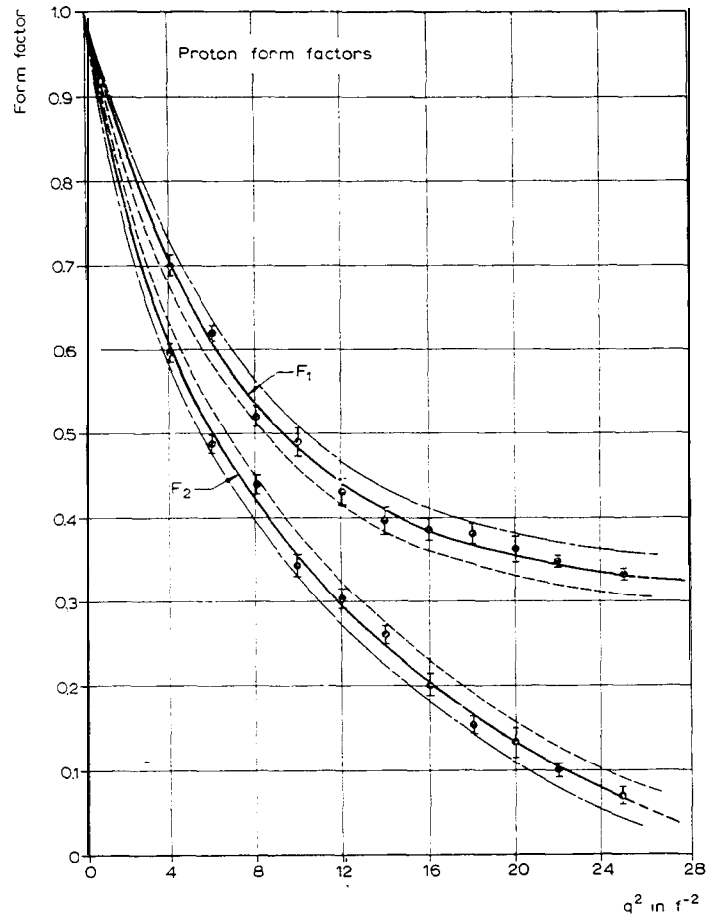

Fig. 10. The most recent Stanford experimental data on the form factors of the proton[17]. There are two dashed curves lying between the *central-value solid experimental lines*. If the error limits are correlated so that they move in opposite directions, as indicated by the *dashed lines*, the corresponding cross sections will still remain consistent with experiment. A similar statement holds for the two *small-dash long-dash curves* lying outside the F_1,F_2 central-value experimental curves. The correlated error question needs additional study but the dashed inner and outer curves are thought to give reasonable error limits of F_1 and F_2.

The early work on the proton was confirmed by subsequent studies at higher energies (~ 600 MeV)[13,14] but these energies were still low enough so that the assumption $F_1 \cong F_2$ could be employed. It was noted in the latter experiments that F_1, was slightly greater than F_2 at values of $q^2 = 4f^{-2}$, where f = fermi = 10^{-13} cm. The value of one fermi corresponds to $(197\ \text{MeV})^{-1}$.

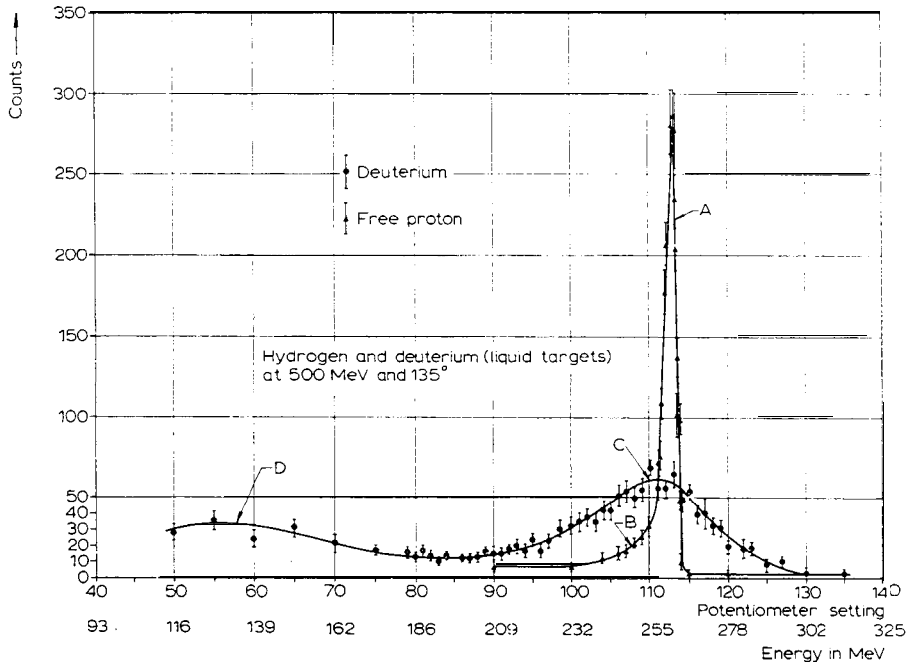

Fig. 11. The experimental comparison of the scattering from the moving proton and neutron in the deuteron (*Curve C*) and the scattering associated with free protons *(Curve A)*[18]. Region *B* shows the bremsstrahlung tail of the proton curve. At *D* are electrons which have been scattered after producing pions in deuterium and also other low-energy electrons. From the scattering data near C the form factors of the neutron can be obtained. The proton peak is used for comparison measurements. No correction has been applied in the figure for the different densities of liquid deuterium and liquid hydrogen.

Recently the extension of the experimental measurements to higher energies (~ 1.0 BeV) showed that indeed $F_1 > F_2$ [15,16]. The appropriate detailed behavior is shown in Fig. 10, and represents the most recent Stanford experimental data on this subject[17]. The possible theoretical significance of these results will be described below, following brief discussions of first, some tests of the Rosenbluth equation and second, the experimental determinations of the form factors of the neutron.

Various tests of the validity of the Rosenbluth equation were made in these experiments by examining whether F_1 and F_2 are really functions of q alone. In all cases studied for which q^2 was less than $25 f^{-2}$ complete consistency in F_1, F_2 values at different energies and angles was observed so that the Rosenbluth equation was checked and found to be valid[17]. At the highest

values reached in these experiments, namely, $q^2 \cong 3\ 1f^{-2}$ the Stanford cross sections could not be combined with the cross sections at the same value of q in recently reported Cornell experiments[24] to give *real* values of F_1 and F_2. If this observation can be confirmed, the possibility exists that quantum electrodynamics may fail at high momentum transfers or that two-proton exchange processes, heretofore neglected, are needed to correct the Rosenbluth equation; or, that some other fundamental aspect of the scattering theory needs improvement. This is an interesting question for the future to decide.

Let us now turn to the question of the neutron. According to relativistic quantum electrodynamics the neutron possesses Dirac and Pauli form factors. Proton and neutron form factors may be referred to respectively as F_{1p}, F_{2p}, F_{1n}, F_{2n}. Static values of the neutron form factors are known to be $F_{1n}(0) = o$, $F_{2n}(0) = 1.00$. F_{1n} is also known from early neutron-scattering experiments to vary as q^4 at small values of q in an expansion of F_{1n} as a function of q^2. This is commonly referred to by saying that within experimental error, the rms radius of the neutron is zero. Thus the neutron is not only a neutral body from the point of view of electric charge, but has a power expansion of F_{1n} that starts off as a function of q^2 with zero slope! Consequently, it is most difficult to determine F_{1n} (and also F_{2n}) of the neutron. The difficulty is compounded by the experimental fact that neutron targets are obtained only by using the deuteron as a neutron carrier, for free neutrons in large numbers are unobtainable in confined spaces. A neutron is in vigorous motion in the deuteron and this additional complication must be taken into account somehow. It is necessary at this point to introduce a relativistic theory of the deuteron to allow properly for the effects of the motion of the bound neutron. Of course, at the present stage of development of relativity theory, the deuteron problem can be solved only in an approximate way. Hence we can see that there are formidable difficulties which face the experimental elucidation and determination of the form factors of the neutron.

Many of these difficulties were overcome in the work of Yearian and the author who used a difference method to compare the scattering from the deuteron and the proton[18]. These investigators first showed that the neutron could not be represented as a point nucleon and that its magnetic moment was distributed in a manner similar to that of the proton. In Fig. 11, we show the type of data from which such conclusions were drawn. The spread-out deuteron peak shows the effect of the motion of the proton and neutron in

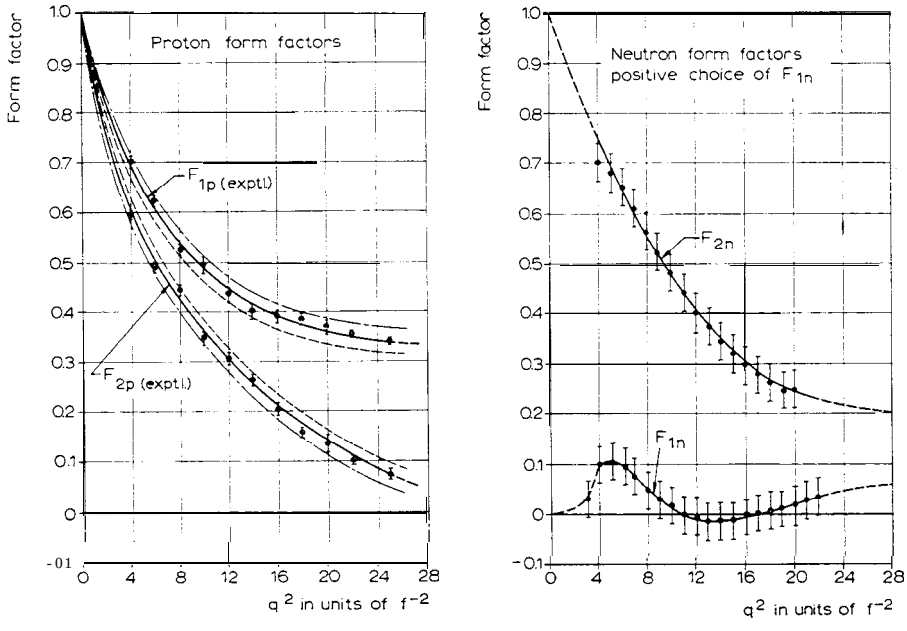

Fig. 12. This figure shows the most recent Stanford results[17,25] for both the neutron and the proton for the positive choice of sign of F_{1n}. The regularity of the neutron curves arises from the fact that the experimental deuteron curves were smoothed before putting the corresponding data into the theoretical formulae from which the form factors are deduced. The four curves of this figure can be fit approximately with dispersion theory or Clementel-Villi curves corresponding to the newly discovered heavy mesons. It is interesting that the newer neutron data agree very well with older result[18] and many of the present conclusions could have been drawn in 1958.

the deuteron and this wide peak may be compared with the sharp peak of the free proton. In the work in which the finite size of the neutron was discovered, the neutron form factor, F_{1n}, was assumed to be approximately zero and F_{2n}, had the behavior described above.

It may be noted parenthetically, that it was on the basis of the above results that Nambu[19] postulated the existence of a new heavy neutral meson, now known as ω-meson. Events of the past year have brilliantly confirmed the existence of this meson[20]. A pion-pion resonance (ρ-meson) responsible for the magnetic behavior of the nucleon form factors was also postulated by Frazer and Fulco[21] on the basis of the above experiments. This resonance was also found recently[22].

The above conclusions about the behavior of the neutron and also the assumption that $F_{1n} \cong 0$, have been confirmed recently[23,24]. More detailed

studies[25], as yet unpublished, support the above description of the neutron form factors. These results are shown in Fig. 12. In Refs. 23 and 24, F_{1n} was found to be small and positive. However Durand[26] has recently shown that the theory of the deuteron used in the early work to derive the values of the neutron form factors can be improved. When the improved formula is employed the slightly positive values of the form factor, F_{1n}, are relatively unaffected in the low q^2 region but in the range $6f^{-2} < q^2 < 2of^{-2}$ the values of F_{1n} are reduced to approximately zero, within experimental error as in Fig. 12[25]. Because the neutron measurements are so fraught with both experimental and theoretical difficulties we must still regard these new, more accurate results, particularly for F_{1n}, as preliminary.

Fig. 12 shows the most recent Stanford results for both the proton[17] and the neutron[25]. An ambiguity exists in the choice of sign of F_{1n}. Fig. 12 shows one choice of the F_{1n} values and the corresponding F_{2n}, values. Fig. 13 shows the neutron data for the other (negative) choice of F_{1n} and the corresponding values of F_{2n} for the negative choice of F_{1n}. Theoreticians prefer the first choice, but as a purely experimental problem the negative F_{1n} values must be considered possible until proved untenable. The dashed parts of the curve refer to probable behavior at low q^2 and in the negative F_{1n} case the steep fall of F_{2n}, would be very surprising and is not expected.

If the first choice of values of F_{1n} is made, which seems much more likely, an understanding of all the proton and neutron data can be obtained along the lines of the heavy-meson or pion-resonance theory of Bergia, *et al*[27]. An interpretation of the early data in terms of Clementel-Villi form factors, using Yukawa clouds of different ranges and delta functions, was also given by the present author and Herman[23]. These initial and approximate theoretical interpretations are probably correct in principle but incomplete in detail and it now seems likely that it is necessary to add to them the effects on the form factors of a third heavy meson (η-meson)[28]. Such a particle has recently been discovered by A. Pevsner, *et al.*[29]. Its existence was also predicted by Sakurai[30].

Attempts are now being made to fit the data of Fig. 12 in terms of the heavy-meson theory in a way similar to that given in Refs. 23 and 27 but now employing three mesons (ϱ, ω, η) instead of only two. I hesitate to show the results of the studies since the exact mass values of the heavy mesons are not yet definite and small variations of these values affect the relative importance of the mesons in the form factor equations in a sensitive way. Furthermore it would not be surprising to find that new heavy mesons are

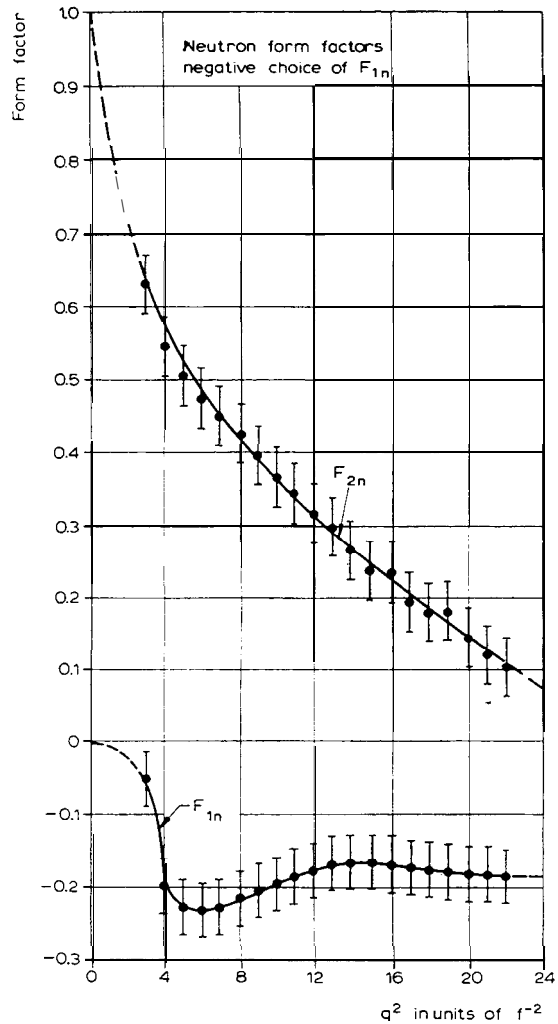

Fig. 13. This figure is similar to the right-hand side of Fig. 12 and gives the set of values of F_{1n} and F_{2n} for the negative choice of F_{1n}. It appears easier at present to fit Fig. 12 with Clementel-Villi curves than Fig. 13.

discovered in the near future, and these might also contribute to the form factors. Suffice it to say that approximate agreement with the data of Fig. 12 can be obtained with the set of three mesons (ϱ, ω, η).

If we now attempt to summarize the recent progress in nucleon structure determinations and in their interpretation, we may say that the proton and neutron are two different aspects of a single entity - the nucleon. The third

component of isotopic spin distinguishes between the two particles. Isotopic form factors can be developed in a well-known way[23] from the proton and neutron form factors. A phenomenological and qualitative interpretation of the nucleon form factors then shows that the same charged mesonic clouds appear in both the neutron and proton. In the proton the clouds add together and in the neutron the clouds cancel, more or less as given in Ref. 23.

It is a bit too early to give the final and definitive details of the mesonic clouds or of their heavy-meson compositions since, as indicated above, such details are now being worked out. However, it is possible, and even likely, that the next year or so should witness a crystallization of the « final » values of the nucleon structure parameters in terms of the models afforded by the new heavy-meson picture of the proton and neutron. The fact that new research is needed in order to clarify this picture is symptomatic of the general problem of the structure of elementary particles.

In concluding this discussion it may be appropriate to return to the theme introduced earlier in the paper and raise the question once again of the deeper, and possibly philosophical, meaning of the term « elementary » particle. As we have seen, the proton and neutron, which were once thought to be elementary particles are now seen to be highly complex bodies. It is almost certain that physicists will subsequently investigate the constituent parts of the proton and neutron - the mesons of one sort or another. What will happen from that point on? One can only guess at future problems and future progress, but my personal conviction is that the search for ever-smaller and ever-more-fundamental particles will go on as long as Man retains the curiosity he has always demonstrated.

The ideas and results presented in this paper represent the work of many individuals. Many of their names are given in the bibliography and I am indebted to them for their important contributions to the subject. I wish to acknowledge my special debt of gratitude to the following individuals who have given me not only invaluable assistance with the many theoretical concepts involved in the fascinating subjects of nuclear and nucleon structure but who have also given me support and encouragement over the last decade: L. I. Schiff, F. Bloch, D. G. Ravenhall, and D. R. Yennie.

1. N. F. Mott, *Proc. Roy. Soc. London,* A 124 (1929) 425; A 135 (1932) 429. (Mott's formula was developed originally in the center of mass frame.)
2. E. Guth, *Anz. Akad. Wiss. Wien, Math.-Naturw. Kl.,* 24 (1934) 299; M. E. Rose, *Phys. Rev.,* 73 (1948) 279; E. Amaldi, G. Fidecaro, and J. Mariani, *Nuovo Cimento, 7* (1950) 757; J. H. Smith, *Ph. D. Thesis,* Cornell University, 1951 (not published); L. I. Shiff, *Phys. Rev., 92* (1953) 988.
3. L. R. B. Elton, *Proc. Phys.* Soc. *London,* A 63 (1950) 1115; 65 (1952) 481; *Phys. Rev.,* 79 (1950) 412; H. Feshbach, *Phys. Rev.,* 84 (1951) 1206; L. K. Acheson, *Phys. Rev.,* 82 (1951) 488; G. Parzen, *Phys. Rev., 80* (1950) 261; 80 (1950) 355.
4. E. M. Lyman, A. O. Hanson, and M. B. Scott, *Phys. Rev.,* 84 (1951) 626.
5. R. Hofstadter, H. R. Fechter, and J. A. McIntyre, *Phys. Rev.,* 91 (1953) 422; *Phys. Rev.,* 92 (1953) 978; R. W. Pidd, C. L. Hammer, and E. C. Raka, *Phys. Rev., 92* (1953) 436.
6. D. R. Yennie, D. G. Ravenhall, and R. N. Wilson, *Phys. Rev., 92* (1953) 1325; 95 (1954) 500; S. Brenner, G. E. Brown, and L. R. B. Elton, *Phil. Mag., 45* (1954) 524; G. E. Brown and L. R. B. Elton, *Phil. Mag.,* 46 (1955) 164; E. Baranger, *Phys.* Rev., 93 (1954) 1127.
7. V. L. Fitch and J. Rainwater, *Phys. Rev., 92 (* 1953) 789.
8. J. H. Fregeau and R. Hofstadter, *Phys. Rev., 99* (1955) 1503.
9. B. Hahn, D. G. Ravenhall, and R. Hofstadter, *Phys. Rev.,* 101 (1956) 1131.
10. R. Hofstadter and R. W. McAllister, *Phys. Rev.,* 98 (1955) 217; R. W. McAllister and R. Hofstadter, *Phys. Rev.,* 102 (1956) 851.
11. M. N. Rosenbluth, *Phys. Rev.,* 79 (1950) 615. See also the reference to a report by L. I. Schiff in this paper, which bears on the problem of proton structure.
12. R. Herman and R. Hofstadter, *High-Energy Electron Scattering Tables,* Stanford University Press, Stanford, California, 1960.
13. E. E. Chambers and R. Hofstadter, *Phys. Rev.,* 103 (1956) 1454.
14. F. Bumiller and R. Hofstadter. See Ref. 12, p. 28; R. Hofstadter, F. Bumiller, and M. R. Yearian, *Revs. Modern Phys., 30* (1958) 482.
15. F. Bumiller, M. Croissiaux, and R. Hofstadter, *Phys. Rev. Letters, 5* (1960) 261; R. Hofstadter, F. Bumiller, and M. Croissiaux, *Phys. Rev. Letters, 5* (1960) 263; R. Hofstadter, F. Bumiller, and M. Croissiaux, *Proc. 1960 Ann. Intern. Conf. High Energy Physics Rochester,* Interscience Publishers, New York, 1960, pp. 762-766.
16. K. Berkelman, J. M. Cassels, D. N. Olson, and R. R. Wilson, Proc. 1960 *Ann. Intern. Conf: High Energy Physics Rochester,* Interscience Publishers, Inc., New York, 1960, p. 757 ff. Also *Nature,* 188 (1960) 94.
17. F. Bumiller, M. Croissiaux, E. Dally, and R. Hofstadter, *Phys. Rev.,* 124 (1961) 1623.
18. M. R. Yearian and R. Hofstadter, *Phys. Rev.,* 110 (1958) 552; *Phys. Rev.,* III (1958) 934; See also, S. Sobottka, *Phys. Rev.,* 118 (1960) 831.
19. Y. Nambu, *Phys. Rev.,* 106 (1957) 1366.
20. B. C. Maglič, L. W. Alvarez, A. H. Rosenfeld, and M. L. Stevenson, *Phys. Rev. Letters,* 7 (1961) 178.
21. W. R. Frazer and J. R. Fulco, *Phys. Rev. Letters,* 2 (1959) 365; *Phys. Rev.,* 117 (1960) 1609. *See also, S.* Drell, *Proc. 1958 Intern. Conf. High Energy Physics CERN,* pp. 27-33.

22. J. A. Anderson, V. X. Bang, P. G. Burke, D. D. Carmony, and N. Schmitz, *Phys. Rev. Letters,* 6 (1961) *365;* A. R. Erwin, R. March, W. D. Walker, and E. West, *ibid,* 628; D. Stonehill, C. Baltay, H. Courant, W. Fickinger, E. C. Fowler, H. Kraybill, J. Sandweiss, J, Sanford, and H. Taft, *ibid, 624.*

23. R. Hofstadter, C. de Vries, and R. Herman, *Phys. Rev. Letters, 6 (1961) 290;* R. Hofstadter and R. Herman, *Phys. Rev. Letters, 6 (1961) 293.*

24. R. M. Littauer, H. F. Schopper, and R. R. Wilson, *Phys. Rev. Letters, 7 (1961)* 141.

25. C. de Vries, R. Hofstadter, and R. Herman, (to be published).

26. L. Durand, III, *Phys. Rev. Letters, 6 (1961)* 631; *Phys. Rev.,* 123 (1961) 1393. See also A. Goldberg, *Phys. Rev.,* 112 (1958) 618.

27. S. Bergia, A. Stanghellini, S. Fubini, and C. Villi, *Phys. Rev. Letters, 6 (1961) 367;* S. Bergia and A. Stanghellini, *Nuovo Cimento,* 21 (1961) 155.

28. C. de Vries, R. Hofstadter, R. Herman, and S. Krasner, *Proc. Aix-en-Provence Conf. Elementary Particles,* Sept. 1961.

29. A. Pevsner, R. Kraemer, M. Nussbaum, C. Richardson, P. Schlein, R. Strand, T. Toohig, M. Block, A. Engler, R. Gessaroli, and C. Meltzer, *Phys. Rev. Letters* (to be published). (I wish to thank Professor Pevsner for communicating his results to me before publication.)

30. J. J. Sakurai, *Phys. Rev. Letters, 7* (1961) 355 and private communication.